Pharmacogn. Mag.
A multifaceted peer reviewed journal in the field of Pharmacognosy and Natural Products
www.phcog.com | www.phcog.net

ORIGINAL ARTICLE

Preparation of Galangin Self-Microemulsion Drug Delivery System and Evaluation of its Pharmacokinetics *in vivo* and Antioxidant Activity *in vitro*

Hao Lu*, Cheng Zhang*, Yuan Liu, Jie Wang, Hanlin Xu

Pharmaceutical Preparation Laboratory, School of Pharmaceutical, Hubei University of Chinese Medicine, No. 1 Huang JiaHu Road West, Hongshan District, Wuhan, China
*These two authors have contributed equally to this work

Submitted: 08-Dec-2021 Revised: 07-Mar-2022 Accepted: 01-Aug-2022 Published: 23-Nov-2022

ABSTRACT

Background: Galangin (Gal) is a natural active flavonoid compound separated from the roots and rhizomes of *Alpinia ofcinarum* Hance. Modern pharmacological studies have shown that Gal has a variety of biological activities such as antitumor, antifungal, antibacterial, antiinflammatory, antiischemic stroke, suppressing vitiligo and Alzheimer's disease, etc., **Objectives:** In this study, our primary goal was to prepare a galangin self-microemulsion drug delivery system (Gal-SMEDDS) and evaluate the effect of free Gal and Gal-SMEDDS on the pharmacokinetic parameters of SD rats, and the protective effect of oxidative damage on human embryonic lung fibroblasts (HFL1) cells *in vitro*. **Materials and Methods:** Gal-SMEDDS was prepared by ethyl oleate, Cremophor CO 40, and PEG-400, and then evaluated by morphology, particle size, zeta potential, polydispersity index, entrapment efficiency, and the pharmacokinetic parameters. The oxidative damage model of HFL1 cells was established by the stimulation of H_2O_2. And the antioxidant effect of Gal-SMEDDS on HFL1 cells was evaluated by ROS fluorescence assay kit and Annexin V-FITC/7-AAD double staining cell apoptosis detection kit. **Results:** The average particle size of Gal-SMEDDS was approximately 21.33 nm, the polydispersity index was 0.096, the zeta potential was – 4.09 mV, and the entrapment efficiency was 96.74%. Compared with free Gal, the release of Gal-SMEDDS was improved *in vitro* release experiment. Cell experiments showed the anti-oxidant effect of Gal-SMEDDS was better than free Gal. *In vivo* pharmacokinetic experiments showed that the pharmacokinetic parameters of Gal-SMEDDS were better than that of free Gal. **Conclusion:** The SMEDDS effectively increased the oral bioavailability of Gal and improved its pharmacokinetic parameters, which were conducive to the anti-oxidant effect of Gal.

Key words: Antioxidant, bioavailability, galangin, HFL1 cells, self-microemulsion drug delivery system

SUMMARY

- We prepared a Gal-SMEDDS which was a light-yellow transparent liquid with small average particle size, narrow distribution and high encapsulation efficiency.
- Gal-SMEDDS could significantly improve the cumulative release rate *in vitro* and pharmacokinetic parameters *in vivo* of free Gal.
- Compared with free Gal, Gal-SMEDDS could better protect HFL1 cells from H_2O_2-induced oxidative damage by reducing the level of ROS and inhibiting the apoptosis of damaged cells.

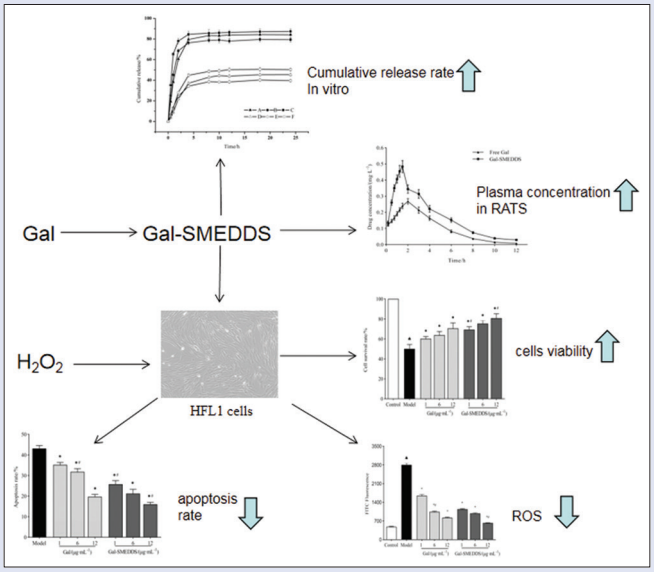

Abbreviations used: Gal: Galangin; Gal-SMEDDS: galangin self-microemulsion drug delivery system; HFL1 cells: Human embryonic lung fibroblasts cells; CCK-8: Cell Counting Kit-8; ROS: reactive oxygen species; HPLC: High performance liquid chromatography.

Correspondence:

Prof. Hanlin Xu,
School of Pharmaceutical, Hubei University of Chinese Medicine; No. 1 HuangJiaHu Road West, Hongshan District, Wuhan - 430065, China.
E-mail: xhl@hbtcm.edu.cn
DOI: 10.4103/pm.pm_567_21

Access this article online
Website: www.phcog.com
Quick Response Code:

INTRODUCTION

Galangin (3,5,7-trihydroxyflavone) is a natural active flavonoid compound, separated from the dried roots and rhizomes of *Alpinia ofcinarum* Hance,[1] a plant of the ginger family, and it also has a higher content in honey, propolis, and golden spirulina.[2] Galangin (Gal) is one of the main active components of *Alpinia ofcinarum* Hance. Modern pharmacological studies have shown that Gal has a variety of biological activities such as antitumor,[3-5] antifungal,[6] antibacterial,[7,8] antiinflammatory,[9-11] antiischemic stroke,[12] suppressing vitiligo,[13] and Alzheimer's disease,[14] etc.[15,16] Recently, there have been reports that

Cite this article as: Lu H, Zhang C, Liu Y, Wang J, Xu H. Preparation of galangin self-microemulsion drug delivery system and evaluation of its pharmacokinetics *in vivo* and antioxidant activity *in vitro*. Phcog Mag 2022;18:1025-34.

Gal has the activity of scavenging oxygen free radicals,[11,17] and shows excellent antioxidant effects. Although Gal has rich pharmacological activities and research prospects, the product development of Gal has some application difficulties: one is that it is insoluble in water and sensitive to factors such as temperature, light, and pH,[18] the other is that it has poor ability to pass the gastrointestinal barrier when administered orally, which limit its clinical application value. Therefore, the use of modern pharmacy methods to modify the dosage form of Gal to improve its bioavailability has an important role in promoting its clinical application and product development.

In the past decades, pharmaceutical researchers have been working on improving the solubility of poorly soluble drugs by many nanotechnological solutions.[19] The SMEDDS, as a very promising nanoformulation, has the advantages of improving drug targeting, bioavailability, and drug pharmacokinetic properties.[20] Specifically, SMEDDS is an isotropic and thermodynamically stable system composed of drug, natural or synthetic oil phases, emulsifiers, and co-emulsifiers. After oral administration, it can spontaneously form O/W microemulsions with a particle size of 10–100 nm under gastrointestinal peristalsis.[21] The formed microemulsions can significantly improve the solubility and oral bioavailability of poorly soluble drugs due to their small particle size and large specific surface area. Because of the above advantages, it has received more attention in the development of oral preparations.[22]

Therefore, in this study, we first prepared a Gal-SMEDDS, and then further evaluated the effect of free Gal and Gal-SMEDDS on the pharmacokinetic parameters of SD rats and the protective effect of oxidative damage on human embryonic lung fibroblasts (HFL1) cells *in vitro*.

MATERIALS AND METHODS

Materials

Gal with a purity of 99% was provided by Aladdin Co. Ltd (Shanghai, China). Ethyl oleate and PEG-400 were purchased from Ruisheng Pharmaceutical Excipients Co. Ltd (Shandong, China). Cremophor CO 40 was bought from Yousuo Chemical Technology Co. Ltd (Shandong, China). Acetonitrile and methanol were purchased from Thermo Fisher Scientific (Waltham, MA). Hydrogen peroxide (H_2O_2) was bought from Damao Chemical Reagent Factory (Tianjin, China). HFL1 cells were purchased from Qishi Co. Ltd (Jiangshu, China). F-12k medium was bought from Jinuo Co. Ltd (Zhengjiang, China). Cell Counting Kit-8 (CCK-8) was bought from biosharp Biotech (Hefei, China). Annexin V-FITC/PI Apoptosis Detection Kit was bought from Beibo Co. Ltd (Shanghai, China). Reactive Oxygen Species (ROS) Assay Kit was bought from Elabscience Co. Ltd (Wuhan, China). Male Sprague Dawley rats were purchased from Changsheng Co. Ltd (6 weeks, Shenyang, China).

HPLC method development

HPLC (LC-20AT, Shimadzu, Japan) was used to quantitative the concentration of Gal with a C_{18} column (4.6 mm × 250 mm, 5 μm, inertstain) at the column temperature of 35°C and the wavelength of 266 nm. The mobile phase was a mixture of methanol and 0.2% phosphoric acid (68:32, *V/V*) at a flow rate of 1 mL/min. The sample was diluted with methanol and the injection volume was 10 μL.

A 5.5 mg Gal reference substance was accurately weighed and placed in a 50 mL volumetric flask, diluted to the scale mark with methanol to obtain 110 μg/mL of Gal stock solution. The Gal stock solution was accurately measured in an appropriate amount and gradually diluted with methanol to obtain 55, 22, 11, 5.5, 2.2, 1.1 and 0.55 μg/mL Gal reference solution. 10 μL Gal reference solution was measured separately and injected into HPLC for methodological investigation of content determination.

Study on solubility of gal in excipients

The solubility of Gal in the different oil phases (soybean oil, IPP, ethyl oleate, oleic acid), different emulsifiers (Cremophor CO 40, Tween-80, EL-40, OP-10) and different co-emulsifier (PEG-400, PEG-200, glycorol, 1,2 - propanediol) was determined. The above different excipients were added to the conical flasks containing excess Gal respectively, placed in a shaker for 24 hr (37°C, 180 r/min). Then centrifuged at 10,000 r/min for 15 min, and 1 mL of the supernatant was taken and diluted with an appropriate amount of methanol. The mass concentration of Gal was measured by HPLC.

Preparation of Gal-SMEDDS

The preparation process of Gal-SMEDDS was optimized by Simplex Lattice Design, Mathematical model fitting and variance analysis, Response Surface Methodology.[23] Specifically, according to the solubility and compatibility experiments, Ethyl oleate, Cremophor CO 40 and PEG-200 were finally selected as the oil phase, emulsifier and co-emulsifier. Gal-SMEDDS was prepared by the following methods: ethyl oleate, Cremophor CO 40, and PEG-400 were precisely weighed and placed in a beaker, and ultrasonic treated for 40 min to make them thoroughly mixed and then stirred in a magnetic stirrer (100 r/min) for 15 min to obtain a blank SMEDDS. Gal was added to the blank SMEDDS at a drug loading of 20 g/kg and mixed with ultrasonication for 40 min. Gal-SMEDDS was obtained by standing at 37°C for 24 hr.

Transmission electron microscopy

Phosphotungstic acid negative staining method was used to observe the morphology of Gal-SMEDDS. Gal-SMEDDS was diluted 10 times with deionized water and mixed with the same amount of 2% phosphotungstic acid for 3 min. The mixed liquid was dropped on a film-coated copper grid and stained for 10 min and then filter paper was used to absorb the excess dye solution. The morphology of the microemulsions was observed under a transmission electron microscope (TEM, JEM-1400, JEOL, and Japan).

Particle size and zeta potential measurement

Gal-SMEDDS was diluted to 10 times with deionized water, and its average particle size, PDI, and Zeta potential were measured by a dynamic light scattering method using the Malvern Nano ZS90 (Malvern, UK). Raw data were collected at 25°C at an angle of 90°, each measurement is performed in triplicate.

Measurement of encapsulation efficiency and drug loading

25 g Gal-SMEDDS was precisely weighed (recorded as W_0) and added in a 25 mL capacity bottle, diluted with deionized water to the scale mark, and shaken to form the microemulsions. 4 mL microemulsions was added in a centrifuge tube and centrifuged for 15 min at 10000 r/min. 0.25 mL supernatant was added in a 25 mL volumetric flask and diluted with methanol to the scale mark. The encapsulated weight of Gal was calculated according to HPLC and recorded as W_1. Another 0.25 g Gal-SMEDDS was precisely weighed and added in a 25 mL capacity bottle, diluted with methanol to the scale mark. The total weight of Gal was calculated according to HPLC and recorded as W_2.

The encapsulation efficiency (EE %) and Drug loading (DL %) were calculated as follows:

$EE\% = W_1/W_2 \times 100\%$. $DL\% = W_1/W_0 \times 100\%$. ($W_2$:the total weight of Gal, W_1:the weight of encapsulated Gal, W_0:the weight of Gal-SMEDDS)

In vitro release study

Dynamic dialysis method,[24] was used to determine the *in vitro* release of free Gal and Gal-SMEDDS in pH = 1.2 artificial gastric juice, pH = 6.8 artificial intestinal juice and deionized water. Briefly, free Gal and Gal-SMEDDS were transferred into pretreated MD44 dialysis bags (molecular weight 8,000–14,000 Da). The dialysis bag was tightened and immersed into a beaker containing 500 mL release medium, respectively. The beakers were placed in a constant temperature water bath shaker (37°C, 100 rpm). The samples of 2 mL were taken at 0.5, 1, 2, 4, 8, 10, 12, 16, and 24 hr and supplemented with an equal volume of fresh dialysis medium. The samples were passed through a 0.45 μm microporous filter membrane. The subsequent filtrates were used as the test product for HPLC and the concentration and cumulative release rate were calculated based on the HPLC results.

Cell culture

HFL1 cells were cultured in F-12K medium (Kaighn's Modification of Ham's F-12 Medium) and incubated at 37°C in a humidified 5% CO_2 atmosphere. HFL1 cells in the logarithmic growth phase were used for cell viability, apoptosis, and ROS detection.

Cell viability

The cells were adjusted to 1×10^5 cells/mL and seeded into 96-well plates according to 100 μL per well and cultured in F-12k medium containing different concentrations of Gal (1, 6, 12, 16, 24, 32, 48 mg/L) in a humidified 5% CO_2 atmosphere at 37°C for 24 hr. Discarding the cell culture medium, 100 μL of F-12k medium containing 10% CCK8 was added to each well and cultured for 4 hr. After that, the absorbance (OD) value at 450 nm was detected in a Model 680 microplate reader ((Bio-Rad, Hercules, CA, USA). Referring to the above experimental procedure, the HFL1 cells were treated with different concentrations of H_2O_2 (100, 200, 300, 400, 500, 600, 700 μmol/L). The concentration of H_2O_2 with 50% cell survival rate was selected as the model concentration of HFL1 cell oxidative damage.

Effects of Gal on HFL1 cell damage caused by H_2O_2

The cells were adjusted to 2×10^5 cells/mL and seeded into 6-well plates according to 1000 μL per well and pre-cultured in F-12k medium containing free Gal and Gal-SMEDDS (1,6,12 mg/L) for 24 hr. Then 525 μmo/L H_2O_2 solution was added and treated for 24 hr. Discarding the cell culture medium, 100 μL of f-12k medium containing 10% CCK8 was added to each well and cultured for 4 hr. After that, the OD value at 450 nm was detected in a Model 680 microplate reader. Untreated cells were considered as the control group and the model group cells were only treated with 525 μmol/L H_2O_2.

HFL1 cell apoptosis detection

The Annexin V-FITC/7-AAD double staining cell apoptosis detection kit was used to detect the effects of free Gal and Gal-SMEDDS on the apoptosis of HFL1 cells. The cells were adjusted to 2×10^5 cells/mL and seeded into 6-well plates according to 1000 μL per well and pre-cultured in F-12k medium containing free Gal and Gal-SMEDDS (1,6, and 12 mg/L) for 24 hr. Then 525 μmol/L H_2O_2 solution was added and treated for 24 hr. The cells were harvested and washed twice in PBS at 4°C, then resuspended with Annexin V binding solution to adjust the density to 1×10^6 cells/mL. Annexin V-FITC staining solution was added to the collected cells and incubated at 2–8°C for 15 min, and 7-AAD staining solution was added for 5 min at 2–8°C. Finally, the blank tube and two single staining tubes were adjusted to compensate the voltage, and the apoptosis rate was detected by flow cytometry. The model group cells were only treated with 525 μmol/L H_2O_2.

Detection of ROS level in HFL1 cells

The ROS fluorescence assay kit (Elabscience Biotechnology Co. Ltd, Wuhan, China, No: 4EYA45VQ76) was used to detect the effects of free Gal and Gal-SMEDDS on the ROS level of HFL1 cells. The cells were adjusted to 2×10^5 cells/mL and seeded into 6-well plates according to 1000 μL per well and pre-cultured in F-12k medium containing free Gal and Gal-SMEDDS (1,6, and 12 mg/L) for 24 hr. Then 525 μmol/L H_2O_2 solution was added and treated for 24 hr. The supernatant was removed and the cells were digested with 0.25% trypsin for 2–3 min and centrifuged at 3,000 r/min for 10 min. The cells were collected and resuspended, and the ROS level was detected by flow cytometry. Untreated cells were considered as the control group and the model group cells were only treated with 525 μmol/L H_2O_2.

In vivo

The pharmacokinetic parameters of free Gal and Gal-SMEDDS in rats were compared after intragastric administration at doses of 50 mg/kg. The male SPF grade SD rats weighing 240 g ± 20 g were raised in the experimental animal center of Hubei University of Chinese Medicine with a standard light (12 hr light/dark) and temperature condition (23 ± 2°C) for one week. All procedures were conducted in accordance with the "Guiding Principles in the Care and Use of Animals" (China) and were approved by the Laboratory Animal Ethics Committee of Hubei University of Chinese Medicine (No: AP20200418). According to the random number table method, the rats were divided into 2 groups, each with 6 rats, and fasted 12 hr before dosing. After one week of adaptive breeding, the free Gal and Gal-SMEDDS were intragastrically administered to each group at the dosage of 50 mg/kg. At 0.17, 0.5, 0.75, 1, 1.25, 1.5, 2, 3, 4, 6, 8, 10, and 12 hr after administration. 0.5 mL blood was collected from the orbital venous plexus of each rat and placed in a centrifuge tube soaked with heparin sodium, and centrifuged at 5,000 r/min for 15 min. The plasma supernatant was immediately separated and stored in a frozen state at −20°C until analyzed. DAS 2.1.1 pharmacokinetic software was used to process the average blood drug concentration data. The main pharmacokinetic parameters include maximum concentration (C_{max}), maximum time (T_{max}), area under the curve ($AUC_{0\text{-}24h}$, $AUC_{0\text{-}\infty h}$), biological half-life ($T_{1/2}$), area under the first moment of the plasma concentration-time curve (AUMC) and mean resident time (MRT).

Statistical analysis

The results were expressed as mean ± standard deviation (SD) of at least three independent experiments. Statistical significance was tested by one-way analysis of variance (ANOVA) by IBM SPSS Statistics 22.0 software. The data had statistical significance when $P < 0.05$.

RESULTS

HPLC method development

According to the chromatographic conditions, the Gal reference solution was injected into the HPLC, and the chromatogram was recorded and shown in Figure 1. Linear regression was performed with the peak area as the ordinate (Y) and the concentration as the abscissa (X). The standard curve equation $Y = 54756X + 659.96$ ($r = 0.999$) was obtained. The results showed Gal has a good linear relationship in the range of 0.55 ~ 110 mg/L. The precision test results showed the precision of the instrument was good (RSD = 1.23%). The stability test results showed that the sample has good stability within 24 hr (RSD = 1.77%). The recovery rate of the sample addition test was 98.97% (RSD = 1.72%), and the results showed that the recovery rate of Gal was good.

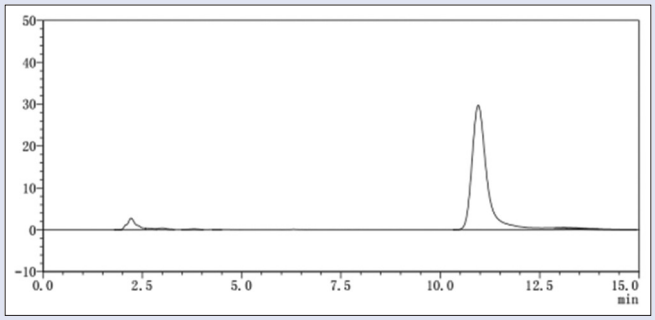

Figure 1: High performance liquid chromatography of Gal

Study on solubility of Gal in excipients

The determination results showed that the solubility of Gal in oil phase was ethyl oleate > IPP > Soybean oil > Oleic acid. The solubility in emulsifier was Cremophor CO 40 > EL-40 > Tween-80 > OP-10. The solubility in co-emulsifier was PEG-400 > PEG-200 > 1,2-Propanediol > Glycerol. The solubility results of Gal in different excipients were shown in Table 1. According to the solubility and compatibility experiments, ethyl oleate, Cremophor CO 40 and PEG-400 were finally selected as the oil phase, emulsifier and co-emulsifier.

Drawing of pseudo-ternary phase diagram

Cremophor CO 40 and PEG-400 were mixed in a mass ratio from 1:9 to 9:1. Then the mixed emulsifier was mixed with ethyl oleate in a mass ratio from 9:1 to 5:5 to obtain the blank SMEDDS. 1 g SMEDDS with different proportions mentioned above was weighed and mixed in a magnetic stirrer (100 r/min), and then slowly added 100 mL deionized water. The respective mass ratio of the ethyl oleate, Cremophor CO 40, and PEG-400 were recorded when forming the microemulsions. The pseudo-ternary phase diagram was drawn by Origin 9.1 software. As shown in Figure 2, in the microemulsion region, the proportion of ethyl oleate, Cremophor CO 40, and PEG-400 were 10%–40%, 25%–80%, and 5%–60%, respectively.

Optimization of Gal-SMEDDS formulation by simplex lattice design

Referring to the result of pseudo-ternary phase diagram and the characteristics of each phase, the mass ratio of each component was determined as follows: ethyl oleate (A) is 10%–40%, Cremophor CO 40 (B) is 30%–60%, and PEG-400 (C) is 30%–60%. Based on this proportion, the average particle size (*Y*1), polydispersity index (PDI) (*Y*2), and drug loading (*Y*3) were chosen as evaluation indexes, and the formulation of the simplex grid method was designed by SLD in design expert 10.0.7.0. The specific mass ratio and evaluation results of each Gal-SMEDDS were shown in Table 2.

Mathematical model fitting and variance analysis

Design Expert 10.0.7.0 software was used to fit the data in Table 2 with the multiple regression model, and the response equation of each index was obtained: $Y_1 = -15.68365A - 1.61872B - 7.14913C + 0.36462AB + 0.95778AC + 0.17863BC - 0.018768ABC$（$r = 0.9998$，$r_{adj} = 0.9997$）；$Y_2 = -7.08296\times10^{-3}A + 3.06837\times10^{-4}B + 3.96818\times10^{-4}C + 1.84966\times10^{-4}AB + 6.89353\times10^{-5}AC - 1.09630\times10^{-4}BC + 5.11937\times10^{-6}ABC$（$r = 0.9825$，$r_{adj} = 0.9675$）；$Y_3 = -4.55377A - 0.74393B - 1.68472C + 0.15378AB + 0.22403AC + 0.067455BC - 6.62669\times10^{-3}ABC$（$r = 0.9937$，$r_{adj} = 0.9882$）. The variance analysis of the above mathematical model was shown in Table 3. The *P* value of each response model was less than 0.0001, which indicated that each index response model has reached a very significant level. The *P* values of the lack of fit were 0.0729, 0.1099, and 0.3919, respectively, which were all greater than 0.05, and the coefficients of regression equation *r* and the coefficient of correction regression equation r_{adj} of each model were greater than 0.95, which indicated that the regression model fitting was successful and representative and can predict the optimal prescription.

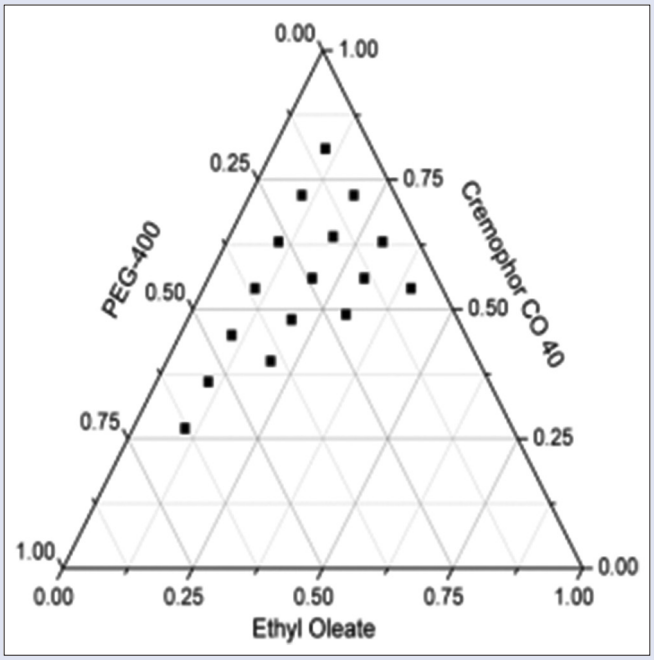

Figure 2: Pseudo-ternary phase diagram of oil phase, emulsifier and emulsifier in Gal-SMEDDS

Table 1: The solubility of Gal in different excipients

Composition	Name	Solubility(g/L)
Oil phase	Soybean oil	0.92±0.13
	IPP	18.16±0.65
	ethyl oleate	29.33±0.87
	Oleic acid	0.61±0.21
Emulsifier	Cremophor CO 40	56.39±1.09
	Tween-80	20.36±0.72
	EL-40	29.38±1.01
	OP-10	13.23±0.64
Co emulsifier	PEG-400	107.68±1.45
	PEG-200	93.18±1.19
	Glycerol	20.83±0.76
	1,2- Propanediol	75.32±1.24

Optimization of prescription by response surface methodology

According to the results of regression analysis, a two-dimensional contour curve and three-dimensional response surface curve of each factor were drawed, and the results were shown in Figure 3. Figure 3a shows that the average particle size decreased with the increase of the proportion of Cremophor CO 40, and increased with the increase of the proportion of ethyl oleate, while PEG-400 had no significant effect on the average particle size. Figure 3b shows that PDI increased with the increase of the proportion of ethyl oleate and decreased with the increase of the proportion of Cremophor CO 40 and PEG-400. Figure 3c shows that the drug loading increased with the increase of the proportion

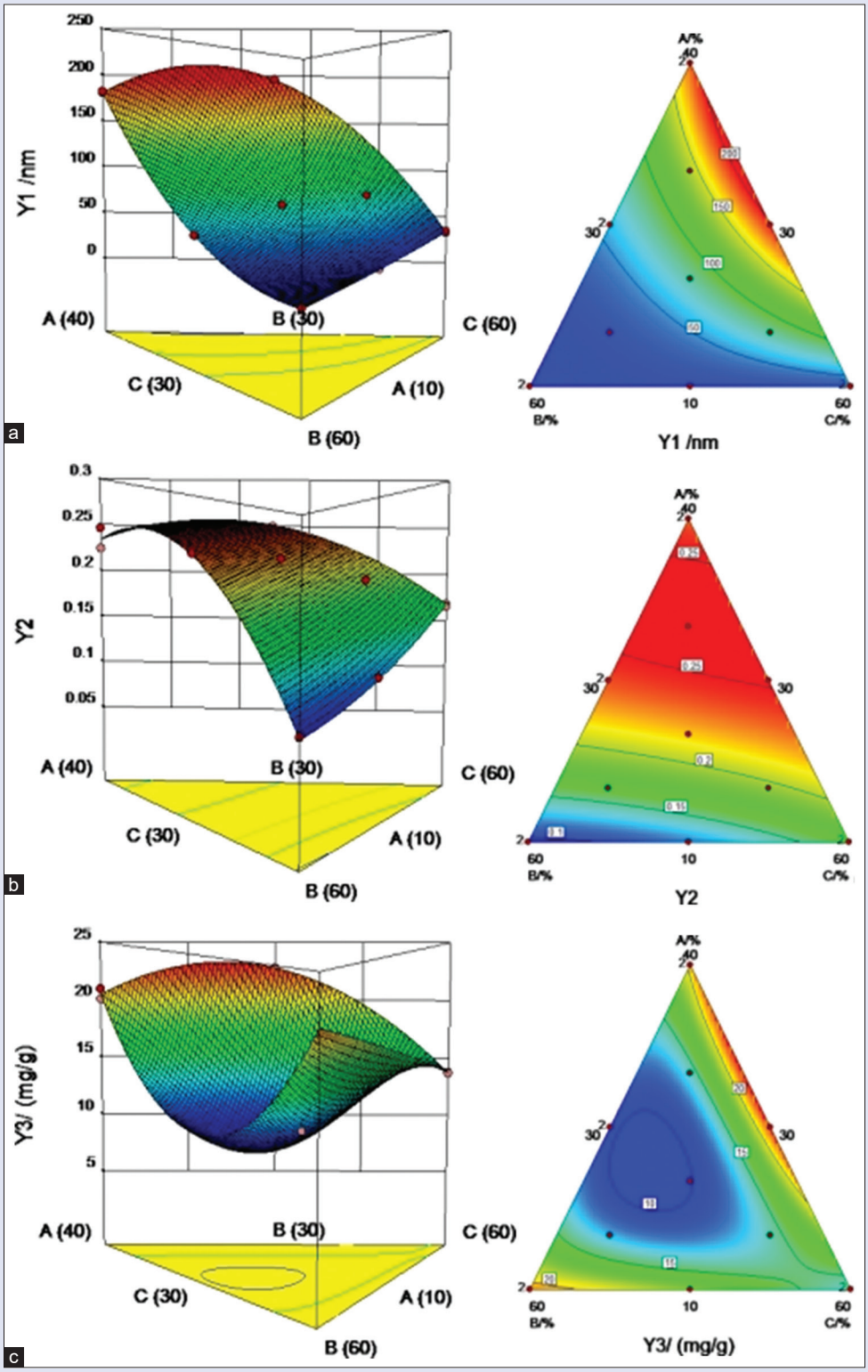

Figure 3: Three dimensional response surface curve, two-dimensional contour curve. (a) Average particle size (b) PDI (c) drug loading

of ethyl oleate and Cremophor CO 40, and increased first and then decreased with the increase of the proportion of PEG-400.

The smaller the average particle size, the larger the specific surface area and the narrower the particle size distribution, which means the faster drug dissolution.[25] The higher the drug loading and the smaller the single dose, which means more conducive to clinical application. Considering the above factors and experimental results, the software predicted that the optimal prescription was W (ethyl oleate): W (Cremophor CO 40): W (PEG-400) = 10%: 60%: 30%, and the average particle size, PDI, and drug loading were 21.376 nm, 0.093, and 20.897 g/kg, respectively. Three batches of Gal-SMEDDS were prepared according to the software prediction, and the average particle size, PDI, and drug loading were

determined to be (21.33 ± 0.62) nm, 0.096 ± 0.003, (21.15 ± 0.32) g/kg, respectively. The deviation between the measured value of each index and the predicted value was small, indicating that the established mathematical model has good predictability.

Preparation of Gal-SMEDDS

In summary, the preparation process of Gal-SMEDDS was as follows: According to the mass ratio W (ethyl oleate): W (Cremophor CO 40): W (PEG-400) = 10%: 60%: 30%, each component were precisely weighed and placed in a beaker, and ultrasonic treated for 40 min to make them thoroughly mixed, then stirred in a magnetic stirrer (100 r/min) for 15 min to obtain blank SMEDDS. Gal was added to the blank SMEDDS at a drug loading of 20 g/kg and mixed with ultrasonication for 40 min. Gal-SMEDDS was obtained by standing at 37°C for 24 hr.

Characterization of Gal-SMEDDS

The morphology of Gal-SMEDDS observed under a transmission electron microscope. As shown in Figure 4, the microemulsions have a round spherical shape with a size within 100 nm. A Malvern Nano ZS90 was used to measure its average particle size, PDI, and zeta potential. As shown in Figure 5, the average particle size, PDI, and Zeta potential of the microemulsions were (21.33 ± 0.62) nm, 0.096 ± 0.003, (−4.09 ± 0.11) mV, respectively, with smaller particle size and narrow distribution.

Drug loading and encapsulation efficiency

The drug loading and encapsulation efficiency of Gal-SMEDDS were calculated. The results showed Gal-SMEDDS has a drug loading capacity of (21.15 ± 0.32) g/kg and an encapsulation efficiency of (96.74 ± 0.25)%.

Table 2: Design and results of simplex grid method for Gal-SMEDDS prescription

A/%	B/%	C/%	Y_1/(nm)	Y_2 (%)	Y_3/(g/kg)
10	30	60	33.87	0.168	13.73
15	50	35	29.15	0.148	11.71
10	60	30	21.04	0.096	21.04
40	30	30	182.37	0.225	20.97
15	35	40	80.98	0.201	14.37
20	40	40	79.81	0.23	10.45
25	45	30	56.93	0.245	10.7
30	35	35	138.14	0.25	13.83
40	30	30	181.43	0.247	20.09
10	45	45	25.13	0.119	17.72
25	30	45	196.57	0.25	22.76
10	60	30	21.82	0.095	20.98
25	45	30	57.45	0.242	10.72
10	30	60	32.62	0.165	13.67

In vitro release study

The release profiles of Gal *in vitro* were summarized. As shown in Figure 6, the cumulative release of Gal-SMEDDS was significantly higher than that of free Gal in different release media. When released *in vitro* for 24 hr, the cumulative release of Gal-SMEDDS and free Gal in deionized water were (87.31 ± 2.52)% and (50.27 ± 1.49)%, respectively; in artificial gastric juice, the cumulative release of Gal-SMEDDS and Gal were (79.37 ± 2.49)% and (39.57 ± 1.29)%, respectively. In artificial intestinal fluid, the cumulative release of Gal-SMEDDS and Gal were (84.14 ± 3.10) % and (45.39 ± 1.28)%, respectively. It showed that SMEDDS can significantly improve the *in vitro* release of Gal.

The effects of Gal on HFL1 viability

The CCK-8 kit was used to detect the cytotoxicity of Gal and H_2O_2 on HFL1 cells, and the results were shown in Figure 7. The results showed that when the concentration of Gal and Gal-SMEDDS was higher than 16 mg/L, it had an inhibitory effect on cell survival. When the concentration was in the range of 1-12 mg/L, HFL1 cells had no obvious cytotoxicity, and the cell survival rate was basically the same. Therefore, 1, 6, 12 mg/L were selected as the concentration for subsequent experiments.

The effects of H_2O_2 on HFL1 viability

The cytotoxicity results of H_2O_2 were shown in Figure 8. The results showed that when the concentration of H_2O_2 was in the range of 500–700 μmol/L, the cell survival rate was significantly decreased ($P < 0.05$), and the inhibitory effect was dose-dependent with

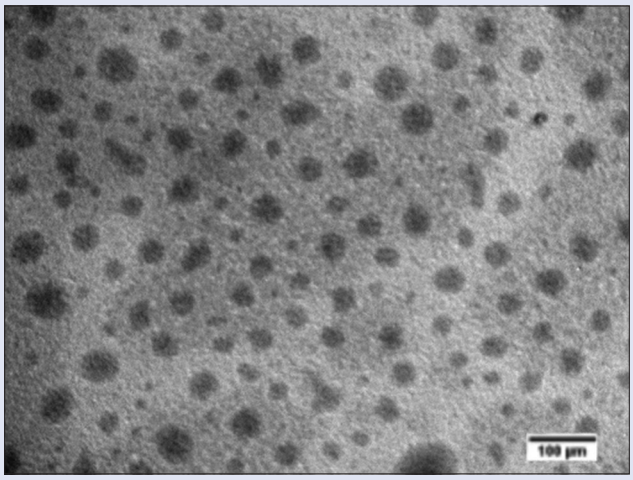

Figure 4: TEM observation images of Gal-SMEDDS (× 30000)

Table 3: Gal-SMEDDS prescription optimization analysis of variance

Source	df	Y_1			Y_2			Y_3		
		Mean square	*F*	*P*	Mean square	*F*	*P*	Mean square	*F*	*P*
Model	6	55578.71	7563.11	<0.0001	0.044	65.52	<0.0001	261.63	183.11	<0.0001
AB	1	2677.11	2185.79	<0.0001	7.793×10^{-3}	69.50	<0.0001	137.83	578.77	<0.0001
AC	1	6556.26	5353.02	<0.0001	2.083×10^{-3}	18.58	0.0035	26.78	112.44	<0.0001
BC	1	3.45	2.82	0.1372	1.437×10^{-4}	1.28	0.2949	0.059	0.25	0.6329
ABC	1	277.91	226.91	<0.0001	2.068×10^{-5}	0.18	0.6805	34.65	145.29	<0.0001
Residual	7	8.57	5.54	0.0658	7.849×10^{-4}	2.83	0.1705	1.67	4.35	0.0947
Lack of fit	3	6.91			5.334×10^{-4}			1.28		
Pure error	4	1.66			2.515×10^{-4}			0.39		
Cor total	13	55587.28			0.045			263.30		

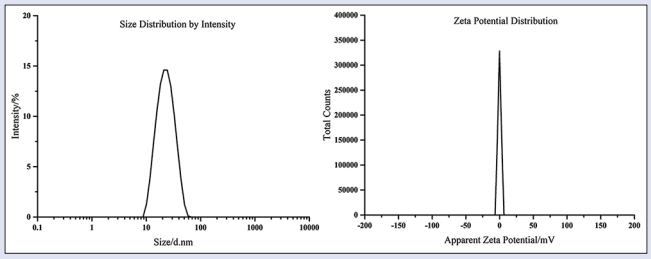

Figure 5: Particle size distribution and apparent zeta potential of Gal-SMEDDS.

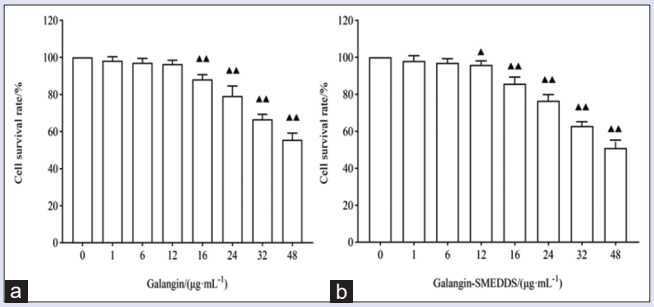

Figure 7: Effects of different concentrations of Gal (a) and Gal-SMEDDS (b) on the viability of HFL1 cells. Compared with the control group, ▲$P < 0.05$, ▲▲$P < 0.01$

the concentration of H_2O_2. GraphPad Prism 8.0 software (GraphPad Software Incorporated, San Diego California USA) was used to fit the relationship between the concentration of H_2O_2 and cell survival. The results showed that the IC_{50} value of H_2O_2 to HFL1 cells was 525 μmol/L, so this concentration was chosen as the modelling concentration.

Effects of Gal on HFL1 viability induced by H_2O_2

The effect of Gal on the viability of HFL1 cells induced by H_2O_2 was shown in Figure 9. The results showed that compared with the control group, the viability of HFL1 cells treated with H_2O_2 was obviously inhibited ($P < 0.05$). Compared with the model group, the viability of cells which pretreated with Gal and Gal-SMEDDS were significantly increased ($P < 0.05$). It showed that both free Gal and Gal-SMEDDS can inhibit the oxidative damage of HFL1 cells induced by H_2O_2, and the Gal-SMEDDS had a more obvious pre protection effect than free Gal ($P < 0.05$).

HFL1 cell apoptosis analysis

The effect of Gal on the apoptosis of HFL1 cells induced by H_2O_2 was shown in Figures 10 and 11. The results showed that the apoptosis rate of HFL1 cells in the model group was 43.10%, while the apoptosis rates of Gal group were 35.20%, 31.80%, and 19.70%, respectively, and those of Gal-SMEDDS group were 25.76%, 21.22%, and 16.04%, respectively. The apoptosis rate of Gal group and Gal-SMEDDS group were lower than that of the model group ($P < 0.05$). These results indicated that free Gal and Gal-SMEDDS can significantly reduce the apoptosis rate of HFL1 cells, and the effect of Gal-SMEDDS was more obvious than that of free Gal.

Detection of ROS level in HFL1 cells

ROS fluorescence kit was used to detect the level of ROS in HFL1 cells induced by H_2O_2. The excitation wavelength of fluorescence was 502 nm, the emission wavelength was 530 nm, and the FITC fluorescence

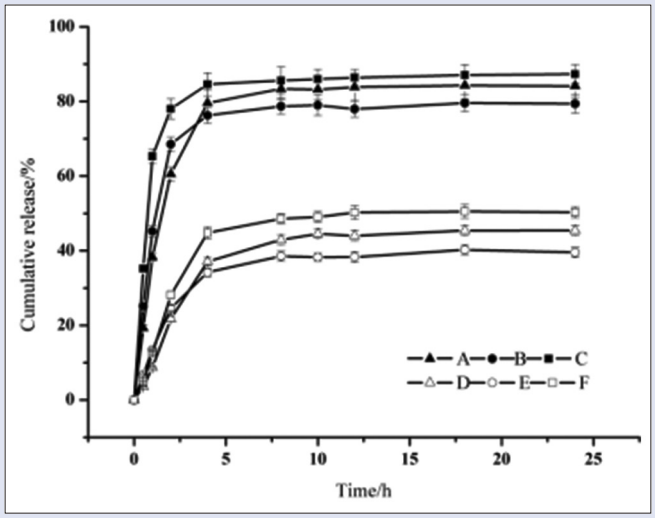

Figure 6: *In vitro* release curves of Gal and Gal-SMEDDS in different media (A) Gal-SMEDDS (pH = 6.8) (B) Gal-SMEDDS (pH = 1.2) (C) Gal-SMEDDS (deionized water) (D) Gal (pH = 6.8) (E) Gal (pH = 1.2) (F) Gal (deionized water)

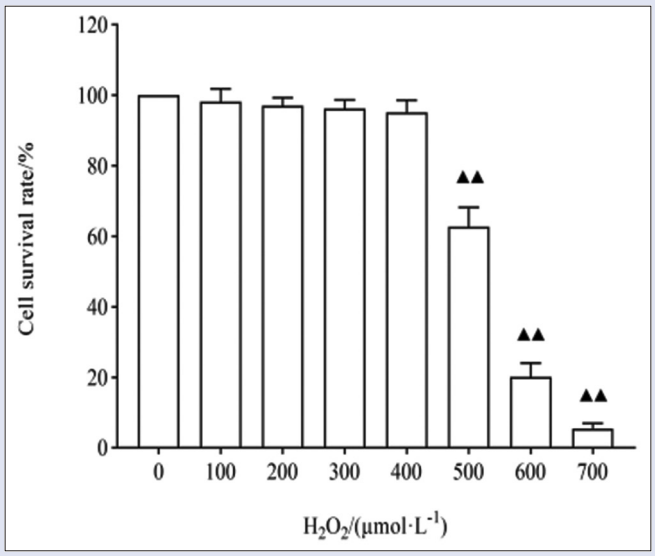

Figure 8: Effects of different concentrations of H_2O_2 on the viability of HFL1 cells. Compared with the control group, ▲▲$P < 0.05$, ▲▲$P < 0.01$

intensity was proportional to the level of ROS in the cell. As it was shown in Figure 12, compared with the control group, the intracellular FITC fluorescence intensity of HFL1 cells treated with H_2O_2 increased significantly, which indicated that H_2O_2 can induce HFL1 cells to release large amounts of ROS. Compared with the model group, the intracellular FITC fluorescence intensity of HFL1 cells decreased after the intervention of Gal and Gal-SMEDDS ($P < 0.05$). The results showed that both free Gal and Gal-SMEDDS can inhibit the release of ROS induced by H_2O_2, and the effect of Gal-SMEDDS was more obvious than that of free Gal.

Pharmacokinetic parameters

According to the method in item "*In vivo*", the samples were prepared at each time point and analyzed by HPLC. The concentration of Gal was calculated and the plasma concentration-time curves of the two

groups were drawn. As it was shown in Figure 13, the absorption degree and speed of Gal-SMEDDS in rats were higher than that of free Gal. DAS 2.1.1 software was used to process the data and showed that both free Gal and Gal-SMEDDS were two-compartment open models. The statistical moment method was used to calculate the pharmacokinetic parameters of the two groups, and the statistical t-test was performed. As it was shown in Table 4, the C_{max}, $AUC_{0\text{-}24h}$, $AUC_{0\text{-}\infty h}$ and MRT of Gal-SMEDDS group were significantly increased, which were 1.74 times, 1.71 times, 1.80 times, and 1.23 times of Gal group respectively. The results indicated that compared with free Gal, Gal-SMEDDS had the advantages of rapid absorption, sufficient absorption, delayed drug release, and can significantly improve the oral bioavailability of free Gal.

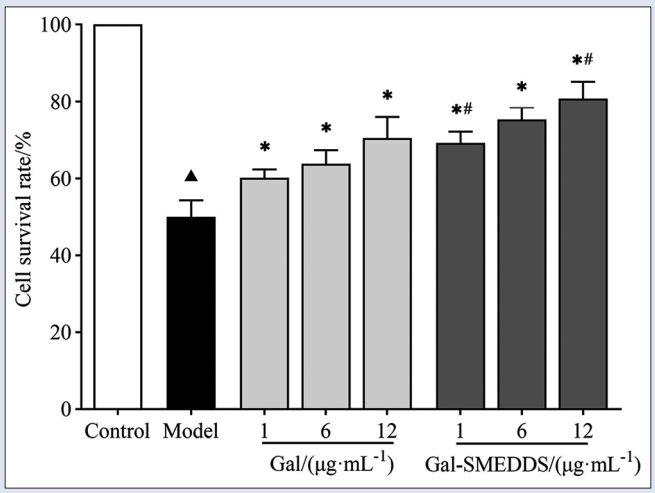

Figure 9: Effect of Gal and Gal-SMEDDS on HFL1 cells viability induced by H_2O_2 (Compared with the control group, $^{▲}P < 0.05$; compared with the model group, $^{*}P < 0.05$; compared with the Gal group, $^{\#}P < 0.05$)

DISCUSSION

As a flavonoid, Gal has a variety of pharmacological activities, such as antiinflammatory, antitumor, antioxidation, antibacterial. However, it is insoluble in water and sensitive to light and pH, resulting in low oral bioavailability and difficulty in product development and application. Therefore, we first used modern pharmacy methods to modify its dosage form and prepared the Gal-SMEDDS.[26] The prepared Gal-SMEDDS was a light-yellow transparent liquid with small average particle size, narrow distribution and high encapsulation efficiency. Then we evaluated the *in vitro* release of the prepared Gal-SMEDDS. The results showed that the cumulative release rate of Gal in Gal-SMEDDS was significantly higher than that of free Gal in different release media, which indicated that SMEDDS had the potential to increase the gastrointestinal absorption rate of Gal and improve the bioavailability of Gal. The reason may be

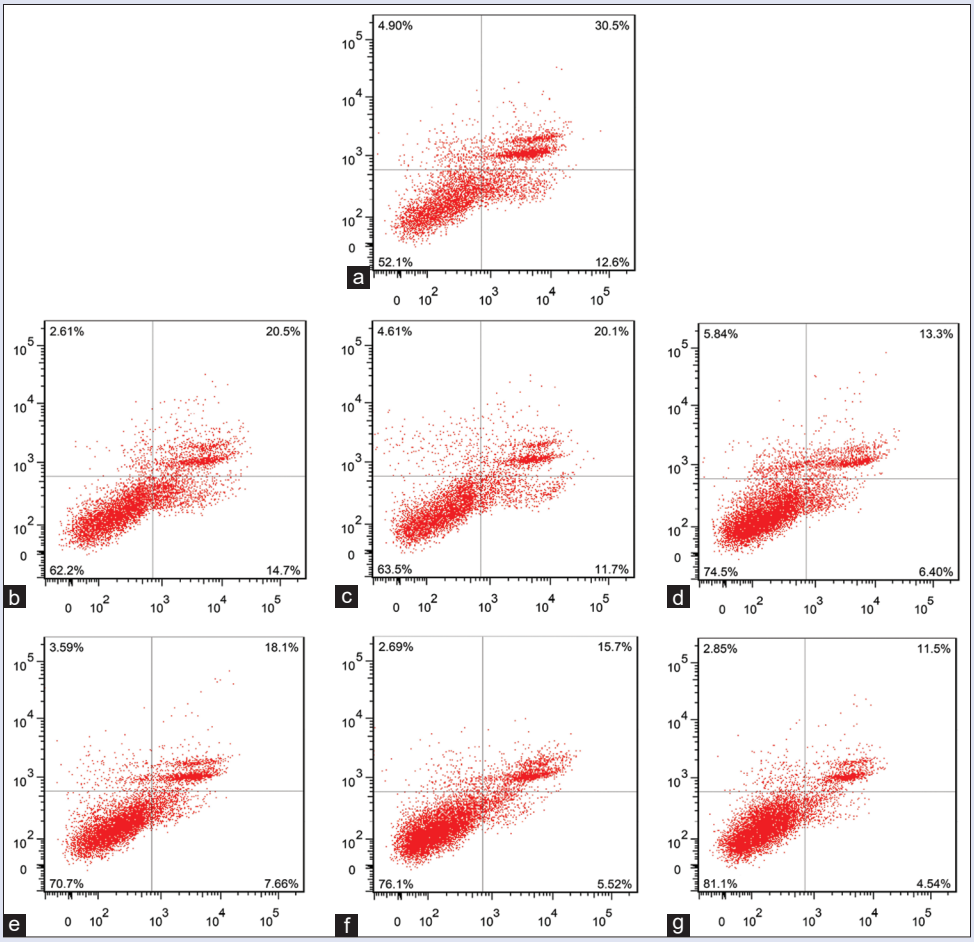

Figure 10: Flow cytometry apoptosis of HFL1 cells in groups. (a) Model group (b) Gal low dose group (c) Gal medium dose group (d) Gal high dose group (e) Gal-SMEDDS low dose group (f) Gal-SMEDDS medium dose group (g) Gal-SMEDDS high dose group

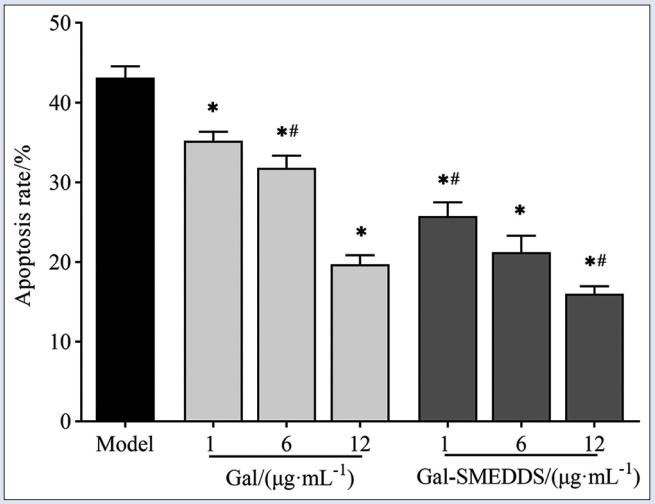

Figure 11: Effect of Gal and Gal-SMEDDS on apoptosis of HFL1 cells. (Compared with the control group, ▲$P < 0.05$; compared with the model group, *$P < 0.05$; compared with the Gal group, #$P < 0.05$)

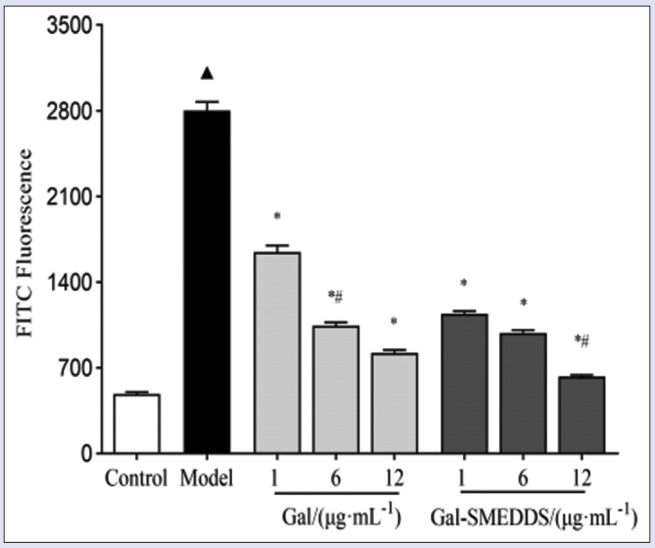

Figure 12: Effect of Gal and Gal-SMEDDS on ROS level in HFL1 cells. (Compared with the control group, ▲$P < 0.05$; compared with the model group, *$P < 0.05$; compared with the Gal group, #$P < 0.05$)

due to the microemulsions formed under mild stirring conditions and the microemulsions had small particle size and large specific surface area, which can help the dissolution of Gal in the medium and accelerate the release of Gal. In addition, Cremophor CO 40, an emulsifier in the formulation, can also improve the drug release rate by increasing the solubility of Gal.

Then the antioxidant effect of Gal-SMEDDS was investigated by cell experiment *in vitro*. Our experimental study found that both Gal and Gal-SMEDDS can inhibit HFL1 cell oxidative damage by reducing ROS level and apoptosis rate. compared with free Gal, Gal-SMEDDS showed better antioxidant effect. The reason may be that the SMEDDS can increase the antioxidant effect of Gal by promoting cell uptake. Finally, we compared the pharmacokinetics of the prepared Gal-SMEDDS and the free Gal. The results of pharmacokinetic studies showed that free Gal and Gal-SMEDDS were both two-compartment open models and

Table 4: Pharmacokinetic parameters after oral administration free Gal and Gal-SMEDDS in rats

Parameters	free Gal	Gal-SMEDDS
$t_{1/2\alpha}$ (h)	1.547±0.108	1.813±0.069#
$t_{1/2\beta}$ (h)	1.646±0.132	3.265±0.300#
t_{max} (h)	1.789±0.074	1.411±0.069#
C_{max} (mg·L^{-1})	0.245±0.016	0.427±0.034#
$AUC_{0\text{-}24h}$ (mg·h·L^{-1})	1.207±0.088	2.059±0.176#
$AUC_{0\text{-}\infty h}$ (mg·h·L^{-1})	1.224±0.091	2.202±0.512#
AUMC (mg·h^2·L^{-1})	4.537±0.252	10.000±0.461#
MRT (h)	3.708±0.146	4.542±0.192#

#$P<0.05$ vs free Gal group

Gal-SMEDDS had a better effect on promoting absorption. We speculated that the reason may be that Gal-SMEDDS forms microemulsions under the peristalsis of the physiological functions of the gastrointestinal tract.[27,28] The small size of the microemulsions was beneficial to the absorption of Gal and can also reduce the enzymatic hydrolysis of Gal in the gastrointestinal tract. In addition, ethyl oleate and Cremophor CO 40 can increase the net absorption of Gal in intestinal epithelial cells and improve the bioavailability of Gal by increasing the cell bypass transport of Gal, enhancing the permeability of cell membrane to Gal, and inhibiting its P-gp efflux.

Nearly 40% of the drugs have the problems of poor solubility and low bioavailability, resulting in their clinical efficacy cannot being fully exerted. Compared with traditional preparations, nano-pharmaceutical preparations present much new pharmacodynamics and metabolic kinetics characteristics and have become the current frontier and hotspot in the international medical field. Gal as a poorly soluble small molecule compound, the main findings of this study provided a pharmaceutical formulations solution for improving the oral bioavailability and the drug ability of Gal, and also provided a research basis and possibility for the further development and clinical application of Gal self-microemulsion oral preparations. In the future, we will carry out the tissue distribution and cellular pharmacokinetic of Gal-SMEDDS to further explore its mechanism of improving bioavailability.

CONCLUSION

In conclusion, a self-microemulsion drug delivery system of Gal was prepared, and its release *in vitro* and pharmacokinetics *in vivo* were evaluated. The results showed that the self-microemulsion drug delivery system can significantly improve the cumulative release rate *in vitro* and pharmacokinetic parameters *in vivo* of free Gal. Cell experiments the anti-oxidant effect of Gal-SMEDDS was better than that of free Gal. This research is helpful to provide an experimental basis for the clinical application of Gal and the development of its nano-preparation products.

Authors' contributions

Hao Lu and Cheng Zhang contributed equally to this work. All authors were involved in the experiments. Lu and Professor Xu was responsible for the design of the experiment. Zhang was responsible for the statistical design. Lu, Zhang, Liu and Wang implemented the experiments. Professor Xu was responsible for the overall coordination of the study.

Financial support and sponsorship

This study was sponsored by the scientific research project of Hubei Provincial Department of Education (NO. B2021118) and Qingmiao Foundation of Hubei University of Chinese Medicine (NO. 2021ZZX010).

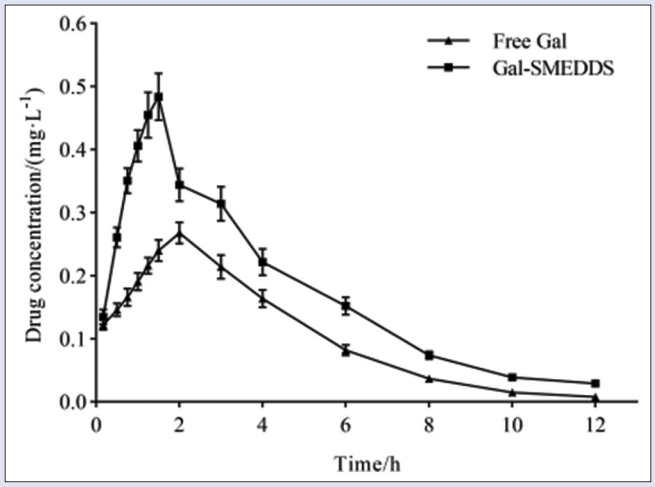

Figure 13: Plasma concentration-time curve of Gal and Gal-SMEDDS in rats at 0-12 h after ig administration

Conflicts of interest

There are no conflicts of interest.

REFERENCES

1. Heo MY, Sohn SJ, Au WW. Anti-genotoxicity of galangin as a cancer chemopreventive agent candidate. Mutat Res 2001;488:135-50.
2. Patel DK, Patel K, Gadewar M, Tahilyani V. Pharmacological and bioanalytical aspects of galangin-a concise report. Asian Pac J Trop Biomed 2012;2:S449-55.
3. Chen D, Li D, Xu XB, Qiu S, Luo S, Qiu E, *et al.* Galangin inhibits epithelial-mesenchymal transition and angiogenesis by downregulating CD44 in glioma. J Cancer 2019;10:4499-508.
4. Yu S, Gong LS, Li NF, Pan YF, Zhang L. Galangin (GG) combined with cisplatin (DDP) to suppress human lung cancer by inhibition of STAT3-regulated NF-κB and Bcl-2/Bax signaling pathways. Biomed Pharmacother 2018;97:213-24.
5. Wang Y, Lin B, Li H, Lan L, Yu H, Wu S, *et al.* Galangin suppresses hepatocellular carcinoma cell proliferation by reversing the Warburg effect. Biomed Pharmacother 2017;95:1295-300.
6. Chudapongse N, Klahan K, Kamkhunthod M, Ratchawong C, Nantapong N. Antifungal activity against Candida albicans and effect on mitochondrial NADH oxidation of galangin. Planta Med 2010;76:415.
7. Ouyang J, Sun F, Feng W, Xie Y, Ren L, Chen Y. Antimicrobial activity of galangin and its effects on murein hydrolases of vancomycin-Intermediate *Staphylococcus aureus* (VISA) strain Mu50. Chemotherapy 2018;63:20-8.
8. Eumkeb G, Sakdarat S, Siriwong S. Reversing β-lactam antibiotic resistance of *Staphylococcus aureus* with galangin from *Alpinia officinarum* Hance and synergism with ceftazidime. Phytomedicine 2010;18:40-5.
9. Wang HB, Huang SH, Xu M, Yang J, Yang J, Liu MX, *et al.* Galangin ameliorates cardiac remodeling via the MEK1/2-ERK1/2 and PI3K-AKT pathways. J Cell Physiol 2019;234:15654–67.
10. Lu H, Yao H, Zou R, Chen X, Xu H. Galangin suppresses renal inflammation via the inhibition of NF-κB, PI3K/AKT and NLRP3 in uric acid treated NRK-52E tubular epithelial cells. BioMed Res Int 2019;2019:3018357.
11. Kim ME, Park PR, Na JY, Jung I, Cho JH, Lee JS. Anti-neuroinflammatory effects of galangin in LPS-stimulated BV-2 microglia through regulation of IL-1β production and the NF-κB signaling pathways. Mol Cell Biochem 2019;451:145-53.
12. Wu C, Chen J, Chen C, Wang W, Wen L, Gao K, *et al.* Wnt/β-catenin coupled with HIF-1α/VEGF signaling pathways involved in galangin neurovascular unit protection from focal cerebral ischemia. Sci Rep 2015;5:16151.
13. Huo SX, Liu XM, Ge CH, Gao L, Peng XM, Zhao PP, *et al.* The effects of galangin on a mouse model of vitiligo induced by hydroquinone. Phytother Res 2014;28:1533-8.
14. Zeng H, Huang P, Wang X, Wu J, Wu M, Huang J. Galangin-induced down-regulation of BACE1 by epigenetic mechanisms in SH-SY5Y cells. Neuroscience 2015;294:172-81.
15. Aloud AA, Chinnadurai V, Chandramohan G, Alsaif MA, Al-Numair KS. Galangin controls streptozotocin-caused glucose homeostasis and reverses glycolytic and gluconeogenic enzyme changes in rats. Arch Physiol Biochem 2020;126:101-6.
16. Kim Y, Lee E, Cho E, Kim D, Kim B, Kang I, *et al.* Protective effects of galangin against UVB irradiation-induced photo-aging in CCD-986sk human skin fibroblasts. Appl Biol Chem 2019;62:40.
17. Duthie G, Morrice P. Antioxidant capacity of flavonoids in hepatic microsomes is not reflected by antioxidant effects *in vivo*. Oxid Med Cell Longev 2012;2012:165127.
18. Sulaiman GM. Molecular structure and anti-proliferative effect of galangin in HCT-116 cells: *in vitro* study. Food Sci Biotechnol 2016;25:247-52.
19. Zhu Y, Wen LM, Li R, Dong W, Jia SY, Qi MC. Recent advances of nano-drug delivery system in oral squamous cell carcinoma treatment. Eur Rev Med Pharmacol Sci 2019;23:9445-53.
20. Yan B, Ma Y, Guo J, Wang Y. Self-microemulsifying delivery system for improving bioavailability of water insoluble drugs. J Nanopart Res 2020;22:18.
21. Mcclements DJ. Nanoemulsions versus microemulsions: Terminology, differences, and similarities. Soft Matter 2012;8:1719-29.
22. Man N, Wang QL, Li HH, Adu-Frimpong M, Sun CY, Zhang KY, *et al.* Improved oral bioavailability of myricitrin by liquid self-microemulsifying drug delivery systems. J Drug Deliv Sci Technol 2019;52:597-606.
23. Sun C, Li W, Zhang H, Adu-Frimpong M, Ma P, Zhu Y, *et al.* Improved oral bioavailability and hypolipidemic effect of syringic acid via a self-microemulsifying drug delivery system. AAPS PharmSciTech 2021;22:45.
24. Yao H, Lu H, Zhang J, Xue XM, Yin C, Hu J, *et al.* Preparation of prolonged-circulating galangin-loaded liposomes and evaluation of antitumor efficacy *in vitro* and pharmacokinetics *in vivo*. J Nanomater 2019;2019:1-9.
25. Galli C. Experimental determination of the diffusion boundary layer width of micron and submicron particles. Int J Pharm 2006;313:114-22.
26. Thomas N, Holm R, Garmer M, Karlsson JJ, Müllertz A, Rades T. Supersaturated self-nanoemulsifying drug delivery systems (Super-SNEDDS) enhance the bioavailability of the poorly water-soluble drug simvastatin in dogs. AAPS J 2013;15:219-27.
27. Goo YT, Song SH, Yeom DW, Chae BR, Yoon HY, Kim CH, *et al.* Enhanced oral bioavailability of valsartan in rats using a supersaturable self-microemulsifying drug delivery system with P-glycoprotein inhibitors. Pharm Dev Technol 2020;25:178-86.
28. Liu J, Wang Q, Omari-Siaw E, Adu-Frimpong M, Liu J, Xu X, *et al.* Enhanced oral bioavailability of bisdemethoxycurcumin-loaded self-microemulsifying drug delivery system: Formulation design, *in vitro* and *in vivo* evaluation. Int J Pharm 2020;590:119887.